JPE 16-6-17

http://dx.doi.org/10.6113/JPE.2016.16.6.2162
ISSN(Print): 1598-2092 / ISSN(Online): 2093-4718

Selection of Voltage Vectors in Three-Level Five-Phase Direct Torque Control for Performance Improvement

Yogesh N. Tatte[†] and Mohan V. Aware[*]

[†,*]Department of Electrical Engineering, Visvesvaraya National Institute of Technology, Nagpur, India

Abstract

This paper presents a Direct Torque Control (DTC) strategy for the five-phase induction motor driven by a three-level five-phase inverter in order to improve the performance of the five-phase induction motor. In the proposed DTC technique, only 22 voltage vectors out of 243 available voltage vectors in a three-level five-phase inverter are selected and are divided in 10 sectors each with a width of 36º. The four different DTC combinations (DTC-I, II, III and IV) for a three-level five-phase induction motor drive are investigated for improving the performance of five-phase induction motor. All four of the DTC strategies utilize a combination of the same large and zero voltage vectors, but with different medium voltage vectors. Out of these four techniques, DTC-II gives the best performance when compared to the others. This DTC-II technique is analyzed in detail for improvements in the performance of five-phase induction motor in terms of torque ripple, *x-y* stator flux and Total Harmonics Distortion (THD) of the stator phase current when compared to its two-level counterparts. To verify the effectiveness of the proposed three-level five-phase DTC control strategy, a DSP based experimental system is build. Simulation and experimental results are provided in order to validate the proposed DTC technique.

Key words: Current distortion, Three-level five-phase DTC, Torque ripple, *x-y* stator flux

I. INTRODUCTION

The Direct Torque Control technique was first introduced in 1986 by Takahashi and Noguchi for three-phase induction motors [1]. This is an actively researched control scheme which can provide a very fast and precise torque response when compared to the scalar and vector control methods. This control scheme has two main drawbacks. The first is the high torque and flux ripples, whereas the second is the variable switching frequency of the devices. Several methods have been proposed to overcome these problems by using modified DTC techniques [2]-[9].

Multilevel inverter topologies are more popular these days in motor-drive systems. These three-level three-phase systems can provide additional controllability over the stator flux and torque due to the availability of 27 voltage vectors.

Manuscript received Dec. 15, 2015; accepted Jul. 1, 2016
Recommended for publication by Associate Editor Gaolin Wang.
[†]Corresponding Author: ytatte@gmail.com
Tel: +91-7709387438, Visvesvaraya National Institute of Technology
[*]Dept. of Electrical Eng., Visvesvaraya Nat'l Institute of Tech., India

After utilizing these voltage vectors in DTC, it is found that the performance of the IM has been significantly improved [10], [11].

Recently, the five-phase induction motor with its inherent advantages has been explored [12]. The five-phase induction motor is normally used for particular applications such as ship propellers drives, aircraft drives and hybrid electrical vehicle drives where the reliability of the overall system is important. The DTC strategy which has shown its superiority over other control techniques is often implemented for five-phase induction motors [13]. After the development of the DTC of five-phase induction motor, research in this area is accelerating to improve its performance [14]-[19].

A DTC controlled five-phase induction motor drive without a speed encoder has been proposed [14], where the virtual voltage vectors are synthesized from large and medium voltage vectors in the *d-q* plane in an aim to nullify low frequency phase current distortion and to achieve full utilization of the dc-bus voltage. The performance of the five-phase IM in the low speed region is also significantly improved by using the DTC technique. In order to reduce the

© 2016 KIPE

demagnetization effect, when the motor runs at a low speed, the classic DTC algorithm has been modified so that the ±72º displaced voltage vectors are replaced with ±36º displaced voltage vectors [15]. Predictive Torque Control (PTC) has been introduced as an alternative to DTC [16], where torque ripple minimization, *x-y* component elimination and improvements in the speed response have been achieved. In [17], the space vector modulation DTC (DTC-SVM) was presented for the five-phase induction motor to cancel the low frequency voltage harmonics. The DTC of a five-phase induction motor having concentrated windings is proposed to enhance the torque producing capability of machines with reductions in torque ripple and current distortion [18], [19]. DTC strategies for dual three-phase permanent-magnet synchronous machines were proposed in [20], [21], wherein the classic DTC strategy is modified to reduce both torque ripple and harmonic current.

The five-phase three-level Space Vector Pulse Width Modulation (SVPWM) technique was proposed [22], where the switching strategy utilizes 113 candidate voltage vectors to develop the desired voltage reference out of an available 3^5 = 243 voltage vectors. This space vector modulation technique increases the space voltage vectors from 32 in two-level to 113 in three-level. When the number of voltage vectors is increased, the freedom to use them for improving a particular problem related to five-phase IMs such as torque ripple, *x-y* stator flux distortion, distortion in the stator current, etc. can be enhanced [23]. The five-phase three-level inverter has shown its capability in improving the performance of five-phase induction motors [24]-[26]. The studies presented in last two decades indicate that five-phase induction motors, when controlled by the classic switching table based DTC (ST-DTC) technique and fed from two-level inverters, suffers from torque ripple, *x-y* stator flux distortion, distortion in the stator current, etc. [13]-[19]. If a five-phase induction motor is controlled by the classic ST-DTC technique and fed from a three-level inverter, the aforementioned problems (torque ripple, *x-y* stator flux distortion, distortion in the stator current, etc.) can be resolved due to the availability of more voltage vectors when compared to the number of voltage vectors in two-level inverters [22]-[26]. Due to the availability of more voltage vectors in three-level inverters, the probability of the selection of optimal voltage vector increases.

In this paper, the performance of the five-phase induction motor is improved in context of torque ripple, *x-y* stator flux and stator current distortion by utilizing a three-level five-phase inverter. Various possible combinations of voltage vectors in a three-level inverter are investigated for torque ripple reduction, *x-y* stator flux elimination and minimization of the stator current distortion. In each combination, 22 voltage vectors are employed through a five-level torque comparator. When the number of voltage vectors in the DTC strategy increases, the complexity in designing the control algorithm also increases. Therefore, the number of voltage vectors employed in each combination is such that a trade-off between the simplicity of the DTC strategy by selecting as minimum possible number of voltage vectors and the freedom of selecting the optimal voltage vectors from a larger number of available voltage vectors. The different combinations proposed in this paper are compared with the classic two-level ST-DTC [13] in order to find a better combination which can improve the performance of the machine in the context of torque ripple, *x-y* stator flux and stator current distortion. Since a three-level inverter or Neutral-Point-Clamped (NPC inverter) is used, the proposed DTC scheme can be used for high-power medium-voltage drive applications. Simulation and experimental results are presented to validate the proposed DTC combinations.

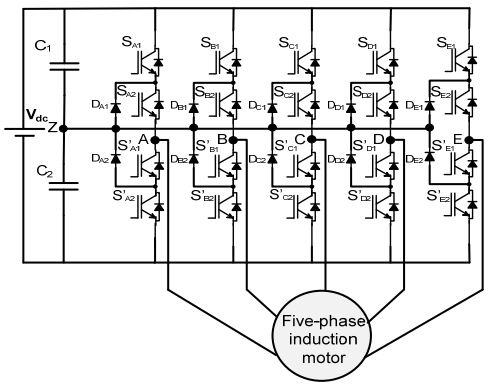

Fig. 1. Three-level five-phase inverter fed five-phase induction motor.

This paper is organized as follows. Section II introduces the DTC strategy for five-phase induction motor driven by a three-level inverter. In section III, an analysis of the torque ripple of the motor is presented. Section IV details the selection of the voltage vectors in the control algorithms. Simulation and experimental results are provided in section V and VI, respectively. Section VII deals with the conclusions from the presented work.

II. THREE-LEVEL FIVE-PHASE DTC

A three-level five-phase inverter fed five-phase induction motor is shown in Fig. 1. The switch function of the three-level five-phase inverter is represented as $S = [S_A\ S_B\ S_C\ S_D\ S_E]^T$. If voltage vector 12101 is selected then $S_A = 1$, $S_B = 2$, $S_C = 1$, $S_D = 0$, $S_E = 1$, where state 2 represents the turning 'ON' of the upper two switches, state 0 represents the turning 'ON' of the lower two switches, and state 1 represents the turning 'ON' of the middle two switches, whereas the remaining switches for a particular state remains 'OFF'. The A phase voltage with respect to the dc-link mid-point 'Z' (pole voltage) is expresses as [23]:

$$V_{AZ} = \frac{S_A - 1}{2} V_{dc} \quad (1)$$

Similarly, the remaining pole voltages can be represented as:

$$V_{BZ} = \frac{S_B - 1}{2} V_{dc} \quad (2)$$

$$V_{CZ} = \frac{S_C - 1}{2} V_{dc} \quad (3)$$

$$V_{DZ} = \frac{S_D - 1}{2} V_{dc} \quad (4)$$

$$V_{EZ} = \frac{S_E - 1}{2} V_{dc} \quad (5)$$

The phase voltages with respect to the load neutral 'N' is expressed in matrix form as [16]:

$$\begin{bmatrix} V_{AN} \\ V_{BN} \\ V_{CN} \\ V_{DN} \\ V_{EN} \end{bmatrix} = \frac{2}{5} \begin{bmatrix} 4 & -1 & -1 & -1 & -1 \\ -1 & 4 & -1 & -1 & -1 \\ -1 & -1 & 4 & -1 & -1 \\ -1 & -1 & -1 & 4 & -1 \\ -1 & -1 & -1 & -1 & 4 \end{bmatrix} \begin{bmatrix} V_{AZ} \\ V_{BZ} \\ V_{CZ} \\ V_{DZ} \\ V_{EZ} \end{bmatrix} \quad (6)$$

The five-phase induction motor drive can be described in two orthogonal and decoupled planes *d-q* and *x-y* as ($\theta = 2\pi/5$):

$$\begin{bmatrix} v_d \\ v_q \\ v_x \\ v_y \\ v_z \end{bmatrix} = \frac{2}{5} \begin{bmatrix} 1 & \cos\theta & \cos 2\theta & \cos 3\theta & \cos 4\theta \\ 0 & \sin\theta & \sin 2\theta & \sin 3\theta & \sin 4\theta \\ 1 & \cos 2\theta & \cos 4\theta & \cos\theta & \cos 3\theta \\ 0 & \sin 2\theta & \sin 4\theta & \sin\theta & \sin 3\theta \\ 1/2 & 1/2 & 1/2 & 1/2 & 1/2 \end{bmatrix} \begin{bmatrix} V_{AN} \\ V_{BN} \\ V_{CN} \\ V_{DN} \\ V_{EN} \end{bmatrix} \quad (7)$$

The zero sequence components (*z*-axis) can be neglected because of the star connection of the windings with an isolated neutral point. The fundamental supply component plus the supply harmonics of the order $10n \pm 1$ (n = 0, 1, 2, 3, . . .) map into the *d-q* plane, and the supply harmonics of the order $10n \pm 3$ (n = 0, 1, 2, 3, . . .) map into the $x-y$ plane, whereas the zero sequence harmonic components ($5n$, with n = 1, 2, 3, . . .) are neglected because of the isolated neutral point [16].

Out of the available 243 voltage vectors in the three-level five-phase space vector topology, only 113 candidate voltage vectors satisfy the required conditions of the phase voltage relationship for the three-level five-phase space vector topology. Therefore, 113 voltage vectors are employed to develop the SVPWM technique [22], [23]. Out of these 113 voltage vectors, 52 voltage vectors are found to be efficient and are used to design the different DTC strategies. The voltage vector numbers from V_1 - V_{10} are large voltage vectors. These voltage vectors are essentially used in combination with the 40 voltage vectors which are medium voltage vector numbers from V_{11} - V_{50} along with the 2 zero voltage vectors (V_0 and V_{51}) to construct the different DTC strategies.

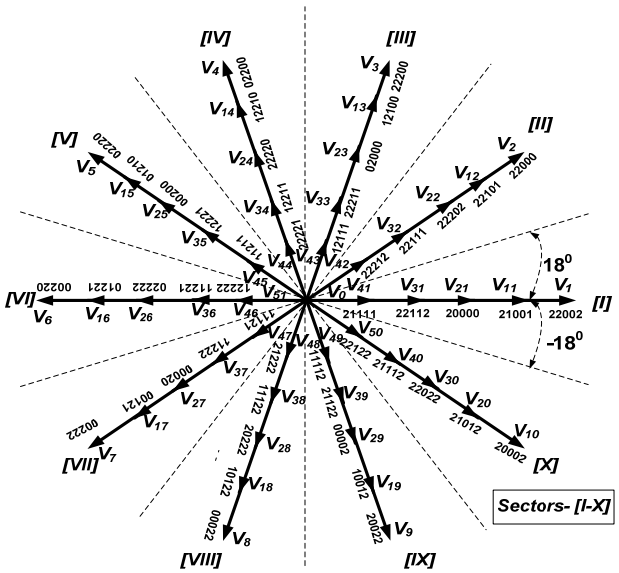

Fig. 2. Voltage vectors mapped in *d- q* space plane.

These 52 voltage vectors are divided into four different groups. These groups are named according to their utilization in building the different DTC schemes. These schemes are named as DTC-I which employs 22 voltage vector numbers from V_1 - V_{10}, V_{11} - V_{20}, V_0 and V_{51}; DTC-II which employs 22 voltage vector numbers from V_1 - V_{10}, V_{21} - V_{30}, V_0 and V_{51}; DTC-III which employs 22 voltage vector numbers from V_1 to V_{10}, V_{31} to V_{40}, V_0 and V_{51}; and DTC-IV which employs 22 voltage vector numbers from V_1 - V_{10}, V_{41} - V_{50}, V_0 and V_{51}. Therefore, each group consists of 22 voltage vectors which include the same 10-large, different 10-medium and the same 2-zero voltage vectors.

The large voltage vectors are compulsorily selected for rapid incrementing of the torque and flux. The selection of the large voltage vectors gives the fast dynamic response of the drive, and the medium voltage vectors help in reducing the torque ripple. Therefore, the groups are formed in view of getting a fast dynamic response and torque ripple reduction through a five-level torque comparator [10], [20], [21]. If the voltage vectors from group number 4 (DTC-IV) are employed to build a DTC control scheme, it will increase the number of switching transition (3, 4) from one switching state to the next. Therefore, the voltage vectors of group number DTC-IV cannot be used to build the DTC strategy. The voltage vectors belonging to the three other groups (DTC-I, II and III) are then used one by one to design the three different DTC strategies. Each of the DTC schemes divides the space vector plane into 10 sectors each with a width of 36º as shown in Fig. 2. The first sector occupies its space in the vector plane from -18º to 18º.

Fig. 2 shows the distribution of the 52 useful voltage vectors in the *d-q* space plane. However, one more space plane, i.e. the *x-y* space plane, exists in five-phase machines which is decoupled and orthogonal to the *d-q* space plane.

There is no coupling of the *x-y* component with the rotor circuit. The electromagnetic torque is produced by the *d-q* component only, and the *x-y* component simply causes losses in the machine. Thus, it becomes necessary to eliminate the magnitude of the *x-y* components. In the proposed DTC control strategies, the *x-y* stator flux elimination algorithm is implemented [15].

III. TORQUE RIPPLE ANALYSIS

The torque ripple of a motor is directly related to the number of levels of the torque controller. When the number of levels of the torque hysteresis controller increases (3-level torque controller to 5-level torque controller), the torque ripple is minimized [10], [20], [21]. Therefore, the five–level torque comparator is designed to avail the utilization of all of the large, medium and zero voltage vectors in order to reduce the torque ripple.

The state variable form of the machine equation in terms of the stator and rotor flux in the stationary reference frame can be expressed in matrix form as [10]:

$$\begin{bmatrix} \frac{d\lambda_s}{dt} \\ \frac{d\lambda_r}{dt} \end{bmatrix} = \begin{bmatrix} -\frac{r_s}{\sigma L_s} & \frac{r_s L_m}{\sigma L_s L_r} \\ \frac{r_r L_m}{\sigma L_s L_r} & j\omega_m - \frac{r_r}{\sigma L_r} \end{bmatrix} \begin{bmatrix} \lambda_s \\ \lambda_r \end{bmatrix} + \begin{bmatrix} 1 \\ 0 \end{bmatrix} V_s \quad (8)$$

Where, L_m is the mutual inductance, L_s is the stator inductance, L_r is the rotor inductance, the leakage coefficient (σ) = $1 - \frac{L_m^2}{L_s L_r}$, λ_s is the stator flux complex vector representing the *d* and *q* axis with $\lambda_s = \lambda_{ds} + j\lambda_{qs}$, λ_r is the rotor flux complex vector representing the *d* and *q* axis with $\lambda_r = \lambda_{dr} + j\lambda_{qr}$, V_s is the stator voltage complex vector representing the *d* and *q* axis with $V_s = V_{ds} + jV_{qs}$, r_s represents the stator resistance, r_r represents the rotor resistance, and ω_m is the motor angular velocity.

The electromagnetic torque can be written as:

$$T_e = \frac{5}{2} P \frac{L_m}{\sigma L_s L_r} \mathrm{Im}\,[\lambda_s . \lambda_r^*] \quad (9)$$

where P is the number of pole pairs and '*' denotes the complex conjugate.

With a small sampling time Δt, the stator and rotor flux at the (k+1)th sampling instant can be written as [2]-[4], [10]:

$$\lambda_{s\,k+1} = \lambda_{s\,k} + \left(-\frac{r_s}{\sigma L_s} \lambda_{s\,k} + \frac{r_s L_m}{\sigma L_s L_r} \lambda_{r\,k} + V_{sk} \right) \Delta t \quad (10)$$

$$\lambda_{r\,k+1} = \lambda_{r\,k} + \left[\frac{r_r L_m}{\sigma L_s L_r} \lambda_{s\,k} + \left(j\omega_m - \frac{r_r}{\sigma L_r} \right) \lambda_{r\,k} \right] \Delta t \quad (11)$$

By substituting (10) and (11) into the discrete form of (9) and simplifying, the electromagnetic torque at the (k+1)th sampling instant can be written as:

$$T_{ek+1} = T_{ek} - T_{ek} \left(\frac{r_s}{L_s} + \frac{r_r}{L_r} \right) \frac{\Delta t}{\sigma} + \frac{5}{2} P \frac{L_m}{\sigma L_s L_r} \left[(V_{sk} - j\omega_{mk} \lambda_{sk}) j\lambda_{rk} \right] \Delta t \quad (12)$$

From (12), it is clear that the torque variation is influenced by the applied voltage vector. If the voltage vector is selected by the DTC control strategy with $V_s = V_{ds} + jV_{qs}$, (12) can be simplified (the subscript k is omitted and the rotor time constant L_r/r_r is negligible when compared to the stator time constant L_s/r_s). The simplified torque equation (12) can be represented in terms of the torque variation (slope), when the large, medium and zero voltage vectors are applied.

When the large voltage vector is applied, the torque increment can be given in term of the slope m_1 as [10]:

$$m_1 = -\frac{T_e r_s}{\sigma L_s} + \frac{5}{2} P \frac{L_m}{\sigma L_s L_r} \left\{ -(v_{ds}\lambda_{qs} + v_{qs}\lambda_{ds}) - \omega_m (\lambda_{ds}\lambda_{dr} + \lambda_{qs}\lambda_{qr}) \right\} \quad (13)$$

When the medium voltage vector is applied, the torque increment can be given in term of the slope m_2 as [10]:

$$m_2 = -\frac{T_e r_s}{\sigma L_s} + \frac{5}{2} P \frac{L_m}{\sigma L_s L_r} \left\{ \frac{1}{2} (v_{ds}\lambda_{qs} - v_{qs}\lambda_{ds}) - \omega_m (\lambda_{ds}\lambda_{dr} + \lambda_{qs}\lambda_{qr}) \right\} \quad (14)$$

It is clearly shown in (13) and (14) that the slopes m_1 and m_2 depend on the length of the applied nonzero voltage vector. Since the zero voltage vector has a zero dc-bus length, the voltage term in (12) becomes zero. Then by simplifying, the torque decrement when the zero voltage vector is applied, can be given in term of the slope m_3 as [10]:

$$m_3 = -\frac{T_e r_s}{\sigma L_s} + \frac{5}{2} P \frac{L_m}{\sigma L_s L_r} \omega_m (\lambda_{ds}\lambda_{dr} + \lambda_{qs}\lambda_{qr}) \quad (15)$$

By applying the zero voltage vector, the torque can be reduced. This is due to the fact that there is no dc-bus available during the time period when the zero voltage vector is applied. With a small sampling time Δt, the slopes m_1, m_2 and m_3 can be considered to be constant, because the dynamics of the speed and flux are not so fast [2]-[4], [10], [20]. Therefore, these slopes can be considered as straight lines as shown in Fig. 5.

IV. SELECTION OF THE VOLTAGE VECTOR

The researches presented up to now emphasizes that the selection of ±72º displaced voltage vectors gives the best dynamic response and helps in improving the performance of five-phase induction motor [13]-[15]. Therefore, when the stator flux lies in sector-I, the voltage vector V_3 is the best suitable voltage vector for rapidly incrementing the torque and flux. The voltage vector is selected for increasing or decreasing the flux (*FI* and *FD*) and torque (*TI* and *TD*). For example, when the stator flux enters the first sector, an increase of the torque (*TI*) and a decrease of the flux (*FD*) are required. Then the voltage vector V_4 is selected as shown in Fig. 3. In Fig. 3, only the selection of large voltage vectors is shown. The medium voltage vector can also be selected depending upon the requirements of the incrementing and

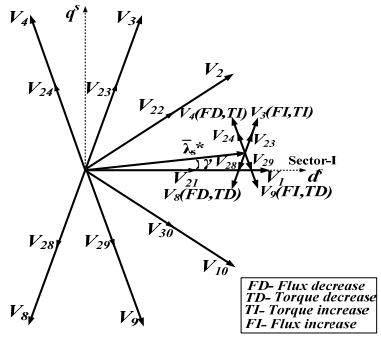

Fig. 3. Voltage vector selection for DTC-II scheme.

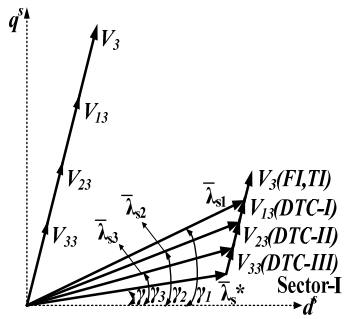

Fig. 4. Performance comparison of DTC-I, DTC-II and DTC-III.

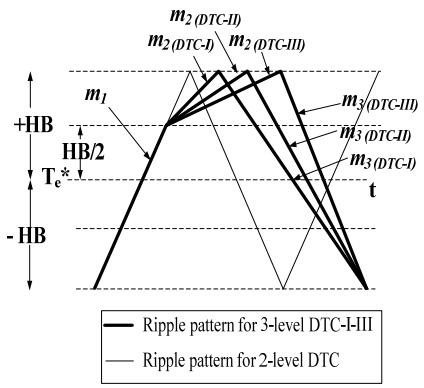

Fig. 5. Torque ripple pattern for three-level five-phase DTC-I-III.

decrementing of the torque and flux.

In Fig. 4, it can be seen that DTC-I has a fast torque response, because $\gamma_1 > \gamma_2 > \gamma_3$ and that it gives the maximum flux, because $\bar{\lambda}_{s1} > \bar{\lambda}_{s2} > \bar{\lambda}_{s3}$ when compared to the DTC-II and DTC-III schemes. Similarly, DTC-II has a moderate torque response and increases the flux, whereas DTC-III negligibly increases the flux and gives a slow torque response when compared to DTC-I and DTC-II. When the motor is started with any of the DTC combinations (DTC-I, II and III) and supposing that the actual torque comes down to the negative full hysteresis band (-HB), the respective large voltage vector is selected to increase the actual developed torque. When the actual torque reaches half of the hysteresis band (HB/2), the voltage vector is changed to the respective medium voltage vector as shown in Fig. 5.

It can be seen from Fig. 5 that DTC-I gives a large torque ripple when compared to DTC-II and DTC-III because it has

TABLE I
VOLTAGE VECTOR SELECTION TABLE FOR DTC-II SCHEME

$d\lambda$	dT	Sector									
		1	*2*	*3*	*4*	*5*	*6*	*7*	*8*	*9*	*10*
1	*2*	V_3	V_4	V_5	V_6	V_7	V_8	V_9	V_{10}	V_1	V_2
	1	V_{23}	V_{24}	V_{25}	V_{26}	V_{27}	V_{28}	V_{29}	V_{30}	V_{21}	V_{22}
	0	V_0	V_{51}	V_0	V_{51}	V_0	V_{51}	V_0	V_{51}	V_0	V_{51}
	-1	V_{29}	V_{30}	V_{21}	V_{22}	V_{23}	V_{24}	V_{25}	V_{26}	V_{27}	V_{28}
	-2	V_9	V_{10}	V_1	V_2	V_3	V_4	V_5	V_6	V_7	V_8
0	*2*	V_4	V_5	V_6	V_7	V_8	V_9	V_{10}	V_1	V_2	V_3
	1	V_{24}	V_{25}	V_{26}	V_{27}	V_{28}	V_{29}	V_{30}	V_{21}	V_{22}	V_{23}
	0	V_{51}	V_0	V_{51}	V_0	V_{51}	V_0	V_{51}	V_0	V_{51}	V_0
	-1	V_{28}	V_{29}	V_{30}	V_{21}	V_{22}	V_{23}	V_{24}	V_{25}	V_{26}	V_{27}
	-2	V_8	V_9	V_{10}	V_1	V_2	V_3	V_4	V_5	V_6	V_7

a fast torque response. DTC-III should give a reduced torque ripple when compared to DTC-I and DTC-II because of its slow torque response. From Fig. 4, it is cleared that if the flux needs to be increased and if the medium voltage vector from DTC-III is selected, the DTC-III cannot increases the stator flux immediately. However, it takes some time to match the stator flux magnitude to its rated value. After reaching to the rated value, the stator flux continues to increase slowly. Once the stator flux error starts crossing the negative flux hysteresis band, a voltage vector is selected which reduces the stator flux. The stator flux continues to decrease. Once the stator flux error starts crossing the positive hysteresis band, the control strategy demands that the flux be increased. Again the DTC-III scheme is unable to fulfill the required demand of immediately incrementing the stator flux. This process of demagnetization continues in DTC-III. This demagnetization causes the torque ripple to be increased when compared to DTC-II [11], [15]. Therefore, due to the slow flux and torque response when compared to DTC-II, DTC-III gives an increased torque ripple. Since the torque and flux response of DTC-II is moderate, demagnetization will not occur and its torque ripple will not be affected. Hence, DTC-II reduces the torque ripple when compared to DTC-I and DTC-III.

Table I depicts the selection of suitable voltage vectors according to the output from the flux comparator, the torque comparator and the location of the *d-q* stator flux for the DTC-II scheme. For example when the stator flux lies in the first sector, if the torque needs to increase rapidly ($dT=2$) and if the flux needs to increase ($d\lambda=1$), a large voltage vector V_3 is selected. The torque comparator is five-level, and the flux comparator is two-level. The operational conditions of the torque and flux comparators are as follows:

$$\lambda_s < \lambda_s^* \quad d\lambda=1 \quad (16)$$

$$\lambda_s^* < \lambda_s \quad d\lambda=0 \quad (17)$$

$$T_e^* - T_e \geq \text{Hysteresis band} \quad dT=2 \quad (18)$$

$$\text{Hysteresis band} > T_e^* - T_e \geq \text{Hysteresis band}/2 \quad dT=1 \quad (19)$$

$$-(\text{Hysteresis band}/2) < T_e^* - T_e < \text{Hysteresis band}/2 \quad dT=0 \quad (20)$$

$$T_e^* - T_e \leq -(\text{Hysteresis band}) \quad dT=-2 \quad (21)$$

$$-(\text{Hysteresis band}) < T_e^* - T_e \leq -(\text{Hysteresis band}/2) \quad dT=-1 \quad (22)$$

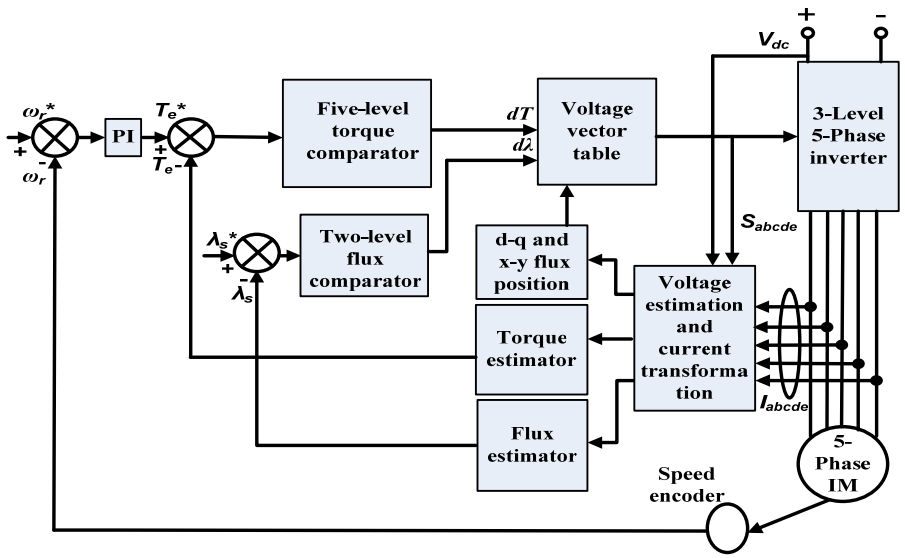

Fig. 6. Control block diagram of three-level five-phase DTC (I–III) schemes.

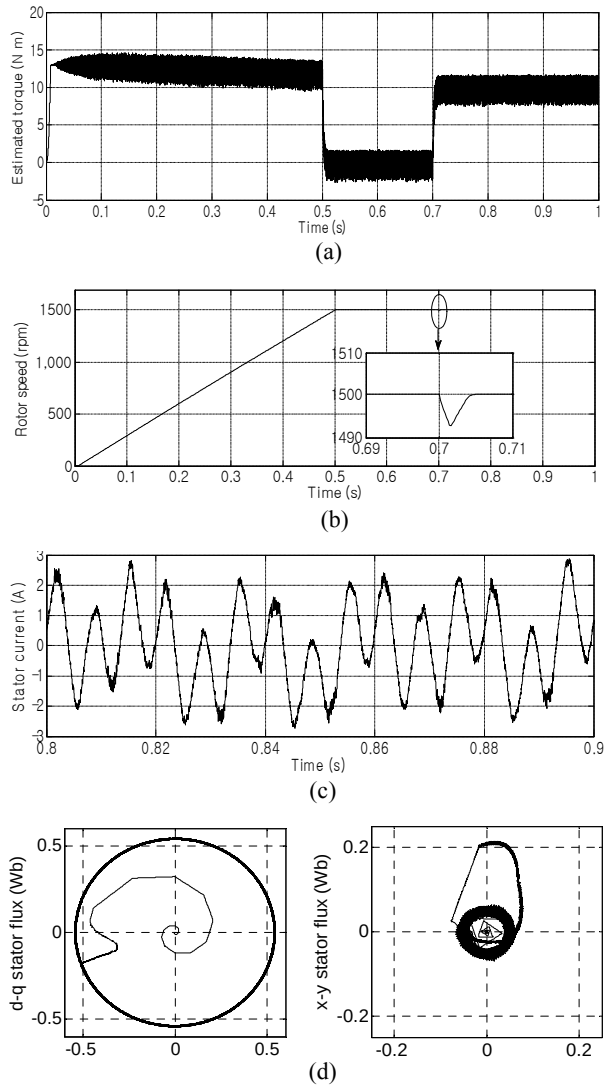

Fig. 7. Simulation results of two-level five-phase DTC, (a) torque response, (b) rotor speed, (c) stator 'a' phase load current and (d) *d-q* and *x-y* stator flux.

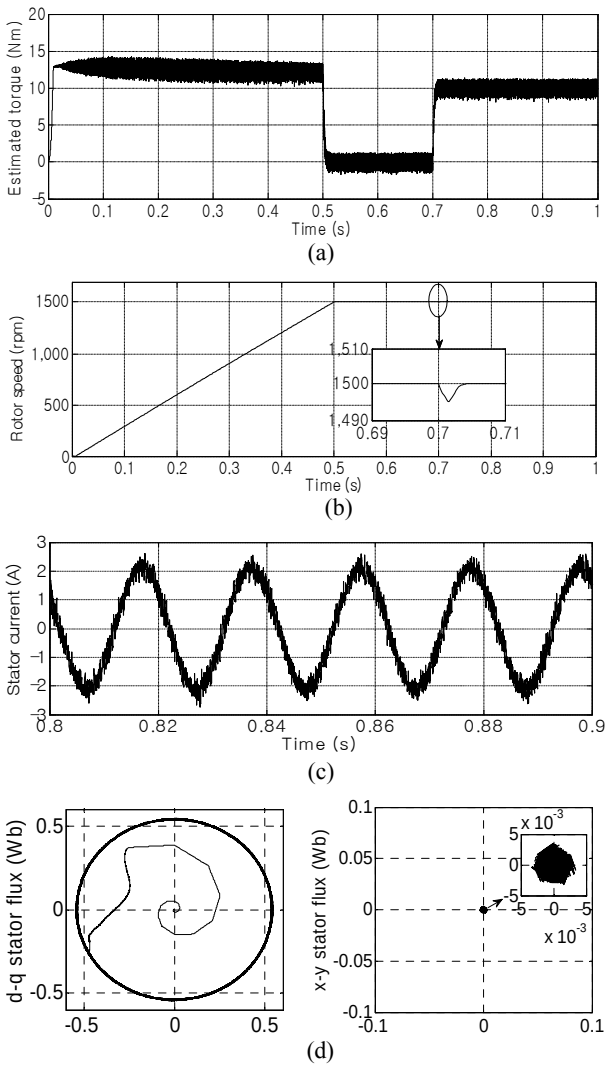

Fig. 8. Simulation results of three-level five-phase DTC-II, (a) torque response, (b) rotor speed, (c) stator 'a' phase load current and (d) *d-q* and *x-y* axis stator flux.

TABLE II
TEST PARAMETERS

Nominal power	1hp
DC Link voltage	400V
Stator Resistance (r_s)	0.8Ω
Rotor Resistance (r_r)	0.6 Ω
Stator leakage inductance (L_{ls})	2.6mH
Rotor leakage inductance (L_{lr})	2.6mH
Mutual Inductance (L_m)	151mH
Rotor Inertia (J)	0.047kg-m^2
Pole pair (P)	2

Fig. 6 shows a block diagram of the DTC scheme for a five-phase induction motor driven by a three-level inverter. This system consists of an outer speed loop, an inner torque loop and a flux loop. Whenever the reference speed command (ω_r^*) is given, the system compares it with the actual speed (ω_r). The error passes through the PI controller which gives the torque reference (T_e^*) for the motor. The reference torque and the reference flux (λ_s^*) are compared with their actual values. Both of the comparators give respective errors which then pass through the hysteresis controllers. The hysteresis controllers for both the flux and the torque give digital outputs (dT and $d\lambda$). Depending upon the digital output from the hysteresis controllers and the *d-q, x-y* stator flux vector position, the voltage vector is selected.

V. SIMULATION RESULTS

The operation of a five-phase induction motor with the proposed DTC schemes is carried out through MATLAB simulations. The five-phase induction motor is driven by a three-level five-phase inverter and is controlled by all of the DTC schemes at a rated speed of 1500 rpm. The rated stator flux and the rated torque of the motor are 0.54 Wb and 13 N-m, respectively. When the motor starts with the rated speed command, the motor torque reaches 13 N-m immediately. The PI controller parameters are set for two-level DTC, DTC-I, DTC-II and DTC-III with Kp = 36, 45, 40 and 63, respectively. Ki for all of the schemes is set to 1. These values are obtained by manual tuning. After some time, the motor gains its reference steady rated speed. At 0.7s, a load torque of 10 N-m is applied to the motor. The hysteresis band of the torque and flux controllers are set to ± 1.538 % of the rated torque and ± 0.55 % of the rated flux, respectively. With these settings of the reference rated speed, the PI controller parameters, the hysteresis bands and the load torque, the proposed three combinations of three-level five-phase DTC (DTC-I, II and III) and the two-level five-phase DTC are simulated with the parameters of the motor detailed in Table II. The sampling frequency of the control system is 30 kHz. The results are taken to demonstrate the performance of a five-phase induction motor controlled by these DTC strategies.

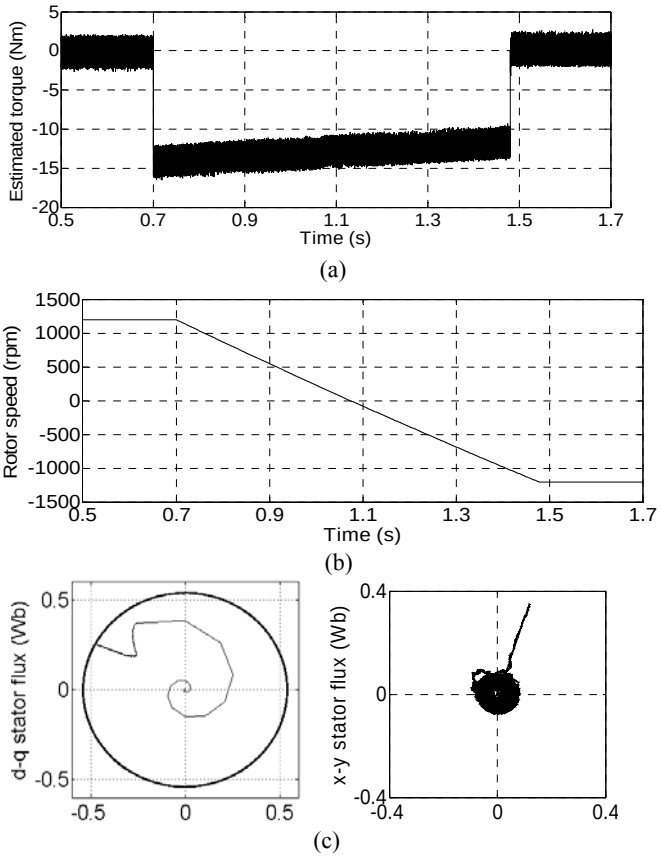

Fig. 9. Simulation results of speed reversal operation of two-level five-phase DTC, (a) torque response, (b) rotor speed and (c) *d-q* and *x-y* stator flux.

Initially, the five-phase induction motor is fed from a two-level five-phase inverter controlled by the classic DTC technique [13]. Fig. 7 shows the performance of the five-phase induction motor, when controlled by the two-level five-phase DTC. The estimated torque of the motor is shown in Fig. 7(a). The load torque is imposed on the motor at 0.7s. The motor follows the reference rated speed of 1500rpm as shown in Fig. 7(b). The motor load current is shown in Fig. 7(c). The *d-q* and *x-y* stator flux trajectories are shown in Fig. 7(d). Since the *x-y* stator flux is not eliminated, the stator current has a significant distortion. Fig. 8 shows the results of the three-level five-phase DTC-II scheme for the same motor. The torque response is indicated in Fig. 8(a). Fig. 8(b) shows the rotor speed response. Fig. 8(c) shows the well regulated stator load current. Fig. 8(d) shows the trajectories of the *d-q* and *x-y* stator flux. It can be seen that the *x-y* stator flux is almost eliminated by the proposed DTC-II scheme. Therefore, the obtained current is well regulated and has a lot less distortion when compared to Fig. 7(c).

Fig. 9 shows the speed reversal operation of the motor, when it is controlled by the two-level DTC. Fig. 9(a) shows the estimated torque with the same torque ripple as in case of the forward rated speed operation of the motor as shown in Fig. 7(a). For this speed reversal operation, the reference

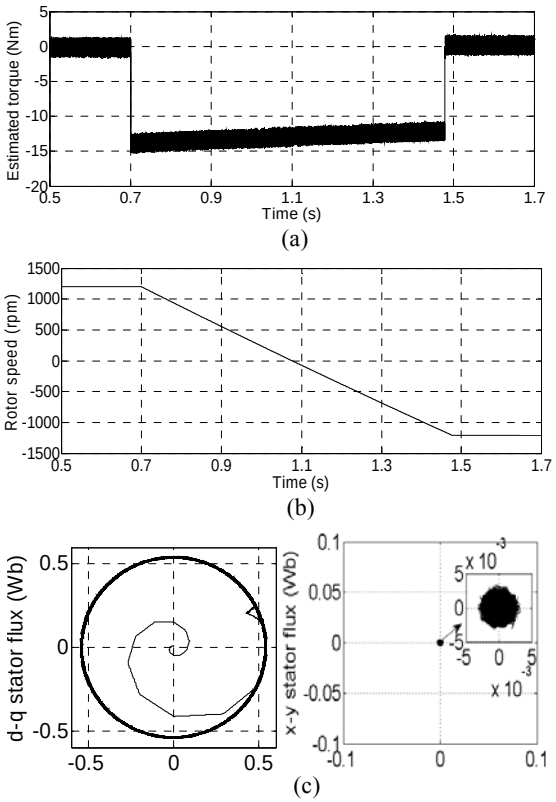

Fig. 10. Simulation results of speed reversal operation of DTC-II, (a) torque response, (b) speed and (c) *d-q* and *x-y* stator flux.

speed command to the motor is 1200 rpm (the medium speed range).

The reverse speed command of -1200 rpm to the motor is given at 0.7s as shown in Fig. 9(b). Fig. 9(c) shows the *d-q* and *x-y* stator flux trajectories. It can be seen that the trajectory of the *d-q* stator flux is well controlled in the circular path with the rated value and that the *x-y* stator flux trajectory has some magnitude. Fig. 10 shows the speed reversal operation of the motor, when it is controlled by the DTC-II technique. Fig. 10(a) shows the estimated torque with the same torque ripple as in case of the forward rated speed operation of the motor as shown in Fig. 8(a). It is clear that the torque ripple minimization with the DTC-II algorithm is also obtained in the speed reversal operation. The rotor speed during this particular speed reversal operation is shown in Fig. 10(b). Fig. 10(c) shows the *d-q* stator flux maintaining its rated value in the air gap. It also shows the *x-y* stator flux which is almost eliminated by the proposed DTC-II algorithm.

The proposed three-level five-phase DTC-II algorithm is designed for the rated, medium and speed reversal operations. The proposed algorithm DTC-II does not reduce the demagnetization during low speed operation. However, the utilization of intermediate voltage vectors (non-vertex vectors) and neglecting the zero voltage vectors in the proposed algorithm in the five-phase three-level inverter can reduce the demagnetization effect during low speed operation as in case of the three-phase induction motor fed by a three-level inverter [11]. However, this is done at the expense of an increase in the torque ripple.

VI. EXPERIMENTAL RESULTS

Fig. 11 shows an experimental setup which consists of a five-phase induction motor, a DSP, an IGBT three-level five-phase inverter with its driver circuit and a signal conditioning circuit including five-current sensors (four are used), a dc-bus voltage sensor and a speed encoder. The inverter is fabricated by using SKM 50GB063D super-fast NPT-IGBT modules and a FRED DSEI 2 x 30 as a clamping diode. The control scheme is based on a TMS320F28027 DSP board. While writing C-codes for the proposed DTC strategy, a five ADC channel (four for the current sensors and one for the dc-bus voltage sensor) signal conditioning circuit, one ePWM to start the conversion from analog to digital and ten GPIO for generating high or low gating signals for the ten modules are used. An experiment is performed for all of the proposed DTC control strategies and the classic two-level DTC strategy with the same parameters detailed in table II. It has been conducted on a symmetrical 1-hp cage-rotor five-phase induction motor. The sampling frequency of the control scheme is 8 kHz. The obtained average switching frequency of the three-level inverter is 2.2 kHz and the two-level inverter is 2.7 kHz. The settings of the PI controller and hysteresis band are same as in the simulation.

Fig. 12 shows experimental results of the rated speed operation of the two-level DTC scheme. Since torque sensors are not used due to their high cost, the estimated torque is obtained from a DSP through a JTAG emulator as shown in Fig. 12 (a). The motor is started from standstill and successfully reaches the rated speed of 1500 rpm as shown in Fig. 12(b). The 'a' phase current, which is highly distorted, is shown in Fig. 12(c) and its THD is shown in Fig. 12(d) which has significant amounts of 3rd and 7th order harmonics. Fig. 12(e) shows the starting current of the motor. Fig. 12(f) shows the *d-q* and *x-y* stator flux. It is observed that the trajectory of the *d-q* stator flux is better controlled in its circular path, whereas the *x-y* stator flux trajectory has a significant magnitude. Due to the presence of the *x-y* stator flux, the stator current obtained in the two-level DTC is highly distorted. Fig. 13 summarizes the experimental results of the proposed DTC-II strategy. Fig. 13(a) shows the estimated torque with its reduced ripple when compared to Fig. 12(a). The motor speed is shown in Fig. 13(b). Fig. 13(c) shows the load current waveform, and its THD is shown in Fig. 13(d). The motor starting current is shown in Fig 13(e). The *d-q* and *x-y* stator flux trajectories for the rated speed operation are shown in Fig. 13(f). It is observed that the trajectory of the *d-q* axis stator flux is better controlled, whereas the *x-y* stator flux trajectory is almost eliminated.

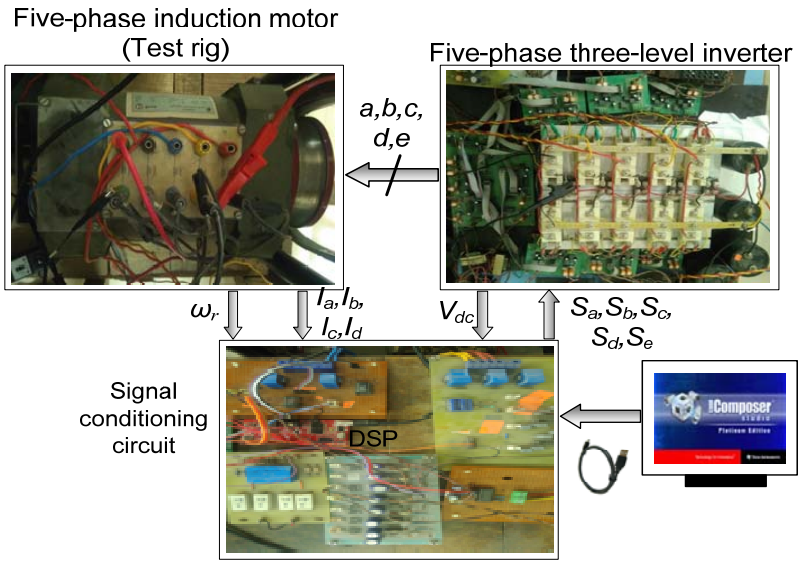

Fig. 11. An experimental set-up of three-level five-phase inverter fed five-phase induction motor controlled by DTC-II technique.

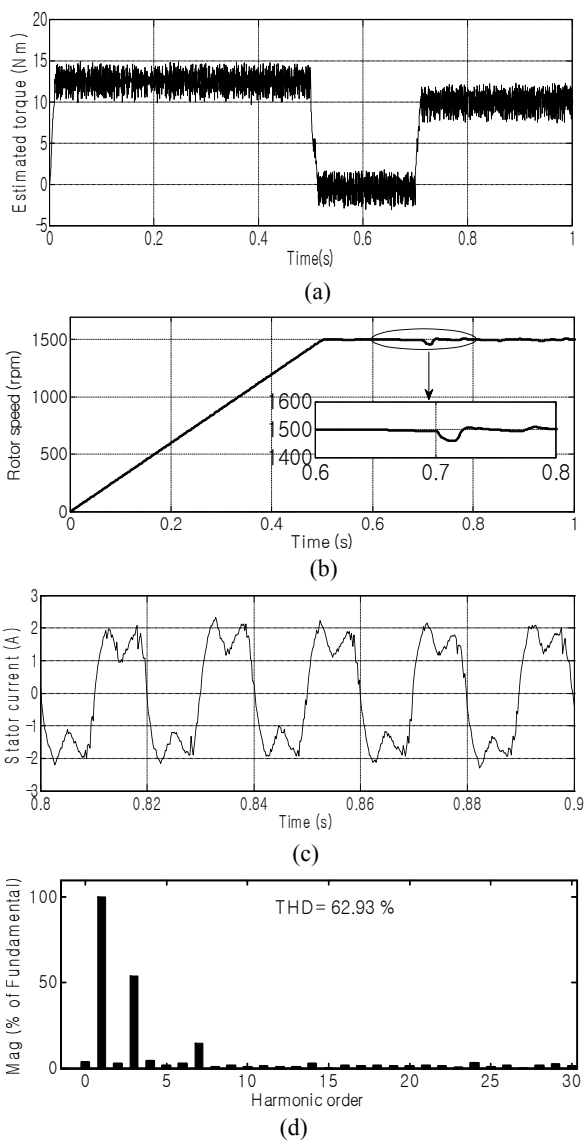

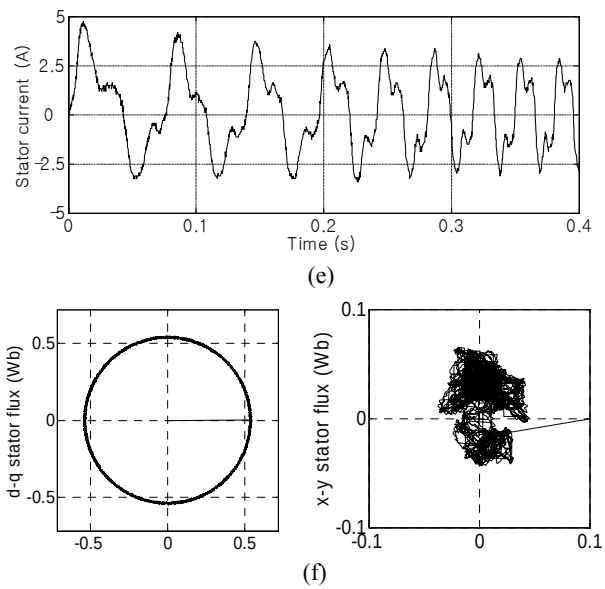

Fig. 12. Experimental results of two-level five-phase DTC, (a) torque response, (b) rotor speed, (c) stator 'a' phase load current, (d) its THD, (e) starting current and (f) trajectories of *d-q* and *x-y* stator flux.

Since the *x-y* stator flux elimination is almost achieved, the current obtained in the DTC-II scheme has a lot less distortion.

Table III and IV show a comparison between all of the presented DTC schemes in terms of the torque ripple, the current THD and the *x-y* stator flux magnitude through simulation and experimental results. It can be observed from both the simulation and experimental results that the DTC-II has reduced the torque ripple by approximately 40% when compared to its two-level counterparts. Since the *x-y* stator flux is almost eliminated in the DTC-II scheme, the current THD is significantly reduced.

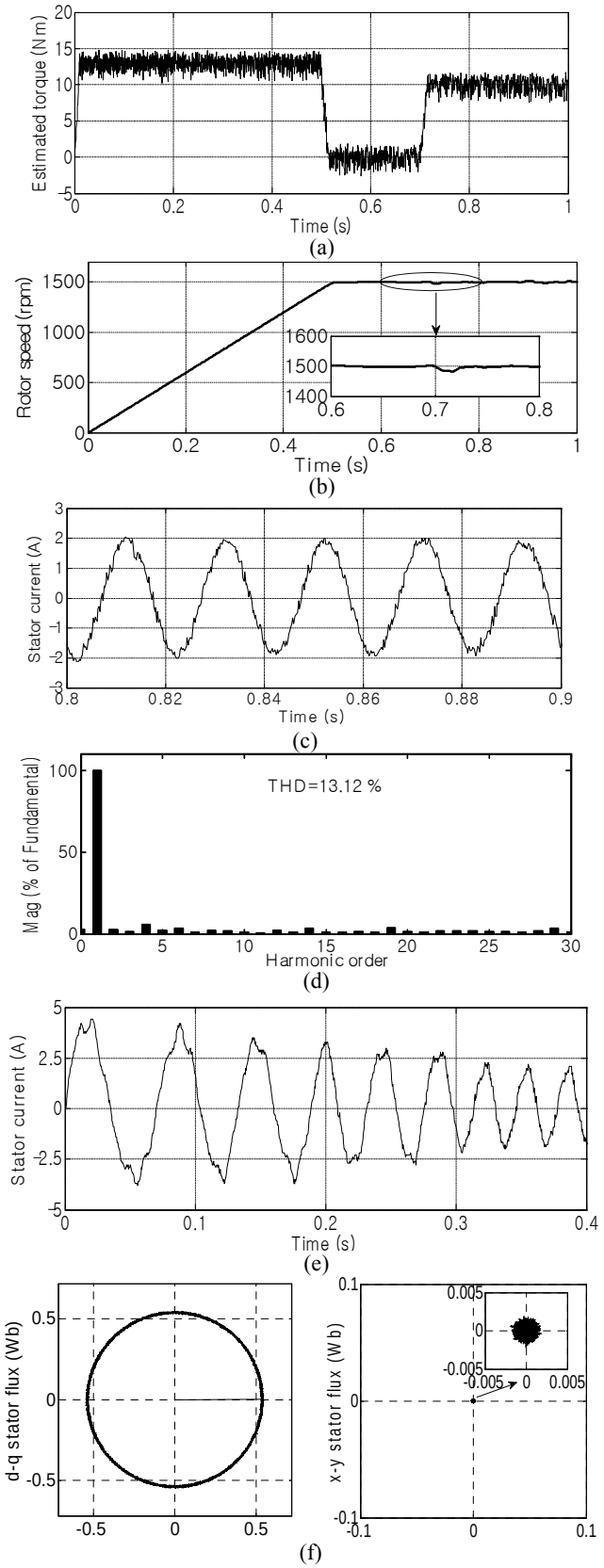

Fig. 13. Experimental results of three-level five-phase DTC-II, (a) torque response, (b) rotor speed, (c) stator 'a' phase load current, (d) its THD, (e) starting current and (f) trajectory of *d-q* and *x-y* stator flux.

TABLE III
SIMULATION DATA OF DIFFERENT SCHEMES

DTC schemes	Peak-peak torque ripple	Current THD (%)	*x-y* stator flux (Wb)
2-L DTC	4.8	91.62	0.063
DTC-I	3.5	22.45	0.0037
DTC-II	2.9	12.65	0.0029
DTC-III	3.6	52.13	0.0041

TABLE IV
EXPERIMENTAL DATA OF DIFFERENT SCHEMES

DTC schemes	Peak-peak torque ripple	Current THD (%)	*x-y* stator flux (Wb)
2-L DTC	5	62.93	0.06
DTC-I	3.6	21.45	0.0032
DTC-II	3.1	13.12	0.0021
DTC-III	3.7	45.48	0.0035

VII. CONCLUSIONS

A Direct Torque Control (DTC) technique for five-phase induction motor fed by a three-level five-phase inverter is proposed to improve the performance of the machine in the context of torque ripple, current distortion and *x-y* stator flux. Four different DTC strategies are investigated to check for the best solution for improving the performance of the five-phase induction motor. From a detailed investigation through simulation and experimental results it is concluded that out of the four different proposed DTC schemes, the DTC-II scheme has the largest improvement in the performance of five-phase induction motor drive. The DTC-II scheme has simultaneously achieved torque ripple reduction, *x-y* stator flux elimination and a reduction in the current distortion by utilizing only 22 voltage vectors out of an available 243 voltage vectors. Hence, it also achieved simplicity in the DTC control scheme.

REFERENCES

[1] I. Takahashi and T. Noguchi, "A new quick response and high efficiency control strategy of an induction motor," *IEEE Trans. Ind. Appl.*, Vol. IA-22, No. 5, pp. 820–827, Sep./Oct. 1986.

[2] D. Casadei, G. Serra, and A. Tani, "Analytical investigation of torque and flux ripple in DTC schemes for induction motors," in *23rd International Conference on Industrial Electronics, Control and Instrumentation (IECON)*, Nov. 1997.

[3] J. K. Kang and S. K. Sul, "New direct torque control of induction motor for minimum torque ripple and constant switching frequency," *IEEE Trans. Ind. Appl.*, Vol. 35, No. 5, pp. 1076–1082, Sep./Oct. 1999.

[4] K. K. Shyu, J. K. Lin, V. T. Pham, M. J. Yang, and T. W. Wang, "Global minimum torque ripple design for direct torque control of induction motor drives," *IEEE Trans. Ind. Electron.* Vol. 57, No. 9, pp. 3148-3156, Sep. 2010.

[5] D. Telford, M. W. Dunnigan, and B. W. Williams, "A novel torque-ripple reduction strategy for direct torque control of induction motor," *IEEE Trans. Ind. Electron.,* Vol. 48, No. 4, pp. 867-870, Aug. 2001.
[6] T. Noguchi, M. Yamamptp, S. Kondo, and I. Takahashi, "High frequency switching operation of PWM inverter for direct torque control of induction motor," in *IEEE Industry Application Society Annual Meeting*, Oct. 1997.
[7] N. R. N. Idris and A. H. M. Yatim, "Reduced torque ripple and constant switching frequency strategy for direct torque control of induction machine," in *15th Annual IEEE Applied Power Electronics Conference and Exposition (APEC)*, Feb. 2000.
[8] A. Jidin, N. R. N. Idris, A. H. M. Yatim, T. Sutikno, and M. E. Elbuluk, "Extending switching frequency for torque ripple reduction utilizing a constant frequency torque controller in DTC of induction motors," *Journal of Power Electronics*, Vol. 11, No. 2, pp. 148-155, Mar. 2011.
[9] S. Arumugam and M. Thathan, "Novel switching table for direct torque controlled permanent magnet synchronous motors to reduce torque ripple," *Journal of Power Electronics*, Vol. 13, No. 6, pp. 939-954, Nov. 2013.
[10] K. B. Lee, J. H. Song, I. Choy, and J. Y. Yoo, "Torque ripple reduction in DTC of induction motor driven by three-level inverter with low switching frequency," *IEEE Trans. Power Electron.*, Vol. 17, No. 2, pp. 255–263, Mar. 2002.
[11] K. B. Lee, J. H. Song, I. Choy, and J. Y. Yoo, "Improvement of low speed operation performance of DTC for three-level inverter fed induction motors," *IEEE Trans. Ind. Electron*., Vol. 48, No. 5, pp. 1006–1014, Oct. 2001.
[12] E. Levi, "Multiphase electric machines for variable-speed applications," *IEEE Trans. Ind. Electron.*, Vol. 55, No. 5, pp. 1893–1909, May 2008.
[13] H. A. Toliyat, H. Xu, and L. J. Peterson, "DSP-based direct torque control (DTC) for five-phase induction machines," *IEEJ Trans. Ind. Appl.*, Vol. 121, No. 12, pp. 1256–1262, 2001.
[14] L. Zheng, J. E. Fletcher, B. W. Williams, and X. He, "A novel direct torque control scheme for a sensorless five-phase induction motor drive," *IEEE Trans. Ind. Electron.*, Vol. 58, No. 2, pp. 503–513, Feb. 2011.
[15] L. Gao, J. E. Fletcher, and L. Zheng, "Low speed control improvements for a 2-level 5-phase inverter-fed induction machine using classic direct torque control," *IEEE Trans. Ind. Electron.*, Vol. 58, No. 7, pp. 2744–2754, Jul. 2011.
[16] J. A. Riveros, F. Barrero, E. Levi, M. J. Duran, S. Toral, and M. Jones, "Variable-speed five-phase induction motor drive based on predictive torque control," *IEEE Trans. Ind. Electron.*, Vol. 60, No. 8, pp. 2957-2968, Aug. 2013.
[17] S. Lu and K. Corzine, "Direct torque control of five-phase induction motor using space vector modulation with harmonics elimination and optimal switching sequence," in *21st Annual IEEE Applied Power Electronics Conference and Exposition (APEC)*, Mar. 2006.
[18] M. H. Kim, N. H. Kim, and W. S. Baik, "A five-phase induction motor speed control system excluding effects of 3rd current harmonics component," *Journal of Power Electronics*, Vol. 11, No. 3, pp. 294-303, Mar. 2011.
[19] N. H. Kim and M. H. Kim, "Modified direct torque control system of five phase induction motor," *Journal of Electrical Engineering and Technology*, Vol. 4, No. 2, pp. 266-271, Jun. 2009.
[20] Y. Ren and Z. Q. Zhu, "Reduction of both harmonic current and torque ripple for dual three-phase permanent-magnet synchronous machine using modified switching-table-based direct torque control," *IEEE Trans. Ind. Electron.*, Vol. 62, No. 11, pp. 6671-6683, Nov. 2015.
[21] Y. Ren and Z. Q. Zhu, "Enhancement of steady-state performance in direct-torque-controlled dual three-phase permanent-magnet synchronous machine drives with modified switching table," *IEEE Trans. Ind. Electron.*, Vol. 62, No. 6, pp. 3338-3350, Jun. 2015.
[22] L. Gao and J. E. Fletcher, "A space vector switching strategy for three-level five-phase inverter drives," *IEEE Trans. Ind. Electron*., Vol. 57, No. 7, pp. 2332–2343, Jul. 2010.
[23] Q. Song, X. Zhang, F. Yu, and C. Zhang, "Research on space vector PWM of five-phase three-level inverter," in *Proceedings of the 8th International Conference on Electrical Machines and Systems (ICEMS)*, Sep. 2005.
[24] B. Sakthisudhursun, J. K. Pandit, and M. V. Aware, "Simplified three-level five-phase SVPWM," *IEEE Trans. Power Electron.*, Vol. 31, No. 3, pp. 2429-2436, Mar. 2016.
[25] S. Payami, R. K. Behera, A. Iqbal, and R. Al-Ammari, "Common-mode voltage and vibration mitigation of a five-phase three-level NPC inverter-fed induction motor drive system," *IEEE Journal of Emerging and Selected Topics in Power Electronics*, Vol. 3, No. 2, pp. 349-361, Jun. 2015.
[26] N. Bodo, O. Dordevic, M. Jones, and E. Levi, "A comparison of three-level single-sided and dual-inverter supply for a five-phase drive," in *15th International Power Electronics and Motion Control Conference (EPE/PEMC)*, Sep. 2012.

Yogesh N. Tatte was born in India, in 1988. He received his B.E. degree in Electrical Engineering from Nagpur University, Nagpur, India, in 2010; and his M.Tech. degree from the Raisoni Engineering College, Nagpur, India, in 2013. He is presently working towards his Ph.D. degree at the Visvesvaraya National Institute of Technology, Nagpur, India. His current research interests include power electronics, electric drives, control and digital-signal-processing-based control applications.

Mohan V. Aware received his B.E. degree in Electrical Engineering from the College of Engineering, Amravati, India, in 1980; his M.Tech. degree from the Indian Institute of Technology, Bombay, India, in 1982; and his Ph.D. degree for his research work on "Direct Torque Controlled Induction Motor Drives" from Nagpur University, Nagpur, India, in 2002. From 1982 to 1989, he was a Design Officer with Crompton Greaves Ltd., Nasik, India. From 1989 to 1991, he was a Development Engineer with Nippon Denro Ispat Ltd., Nagpur, India. From 2001 to 2002, he was a Research fellow with the Electrical Engineering Department, Hong Kong Polytechnic University, Hong Kong, China. He is presently working as a Professor in the Department of Electrical Engineering, Visvesvaraya National Institute of Technology, Nagpur, India. He has published more than 100 technical papers in different journals and conference proceedings. His current research interests include electrical drives, distributed generation, energy storage systems and power electronics. He is a Commonwealth Academic Fellow.